Brian Corey et al.: Antenna Cross-Polarization Characteristics at Geodetic VLBI Stations, IVS 2006 General Meeting Proceedings, p.157–161
http://ivscc.gsfc.nasa.gov/publications/gm2006/corey

# Antenna Cross-Polarization Characteristics at Geodetic VLBI Stations

*Brian Corey, Michael Titus*

*MIT Haystack Observatory*
*Contact author: Brian Corey, e-mail:* bec@haystack.mit.edu

**Abstract**

We describe the design, analysis, and preliminary results of observations carried out in July 1996 to measure the S/X-band cross-polarization response of the nominally right-circularly-polarized (RCP) feeds at geodetic antennas. At VLBA sites the left-circular (LCP) response is typically –22 to –28 dB relative to RCP, and always <–20 dB. Cross-polarization is significantly higher at some non-VLBA sites, with values of –20 to –15 dB at X-band. Corresponding errors in the X-band multiband delays due to the cross-polarization are of order 5–10 ps over 360 MHz on baselines to non-VLBA sites.

## 1. Introduction

A major source of instrumental error in geodetic VLBI is cross-polarization in the nominally right-circularly-polarized (RCP) antenna feeds [4]. For two antennas observing with imperfect RCP feeds, the interferometric signal on an unpolarized source, normalized relative to the response to a purely RCP source, is [1, 3]:

$$\frac{R_1 R_2^* \,(\text{unpol source})}{R_1 R_2^* \,(\text{pure RCP source})} \;=\; 1 + D_{1R}\, D_{2R}^*\, e^{2i(\phi_1-\phi_2)} \tag{1}$$

where $D_{iR}$ is the LCP leakage term for the station $i$ RCP feed given by the L/R complex ratio between the feed voltage responses to the two $E$-field polarization senses, and $\phi_i$ is the feed rotation angle (which, in the case of an alt-az antenna mount, is the parallactic angle). The group delay error $\tau_L$ caused by the LCP contamination is the partial derivative with respect to frequency of the argument of equation (1). For weak cross-polarization ($|D_{1R}D_{2R}^*| \ll 1$), $\tau_L$ reduces to the frequency derivative of the imaginary component and can be expressed as the sum of two terms:

$$\tau_L = A\,\cos 2(\phi_1-\phi_2) \;+\; B\,\sin 2(\phi_1-\phi_2) \tag{2}$$

Because $\tau_L$ depends on feed rotation angle, it varies with pointing direction for all but equatorial-mount antennas, and hence is correlated with geometry. In general, the delay errors do not close around a triangle of stations.

The level of LCP contamination at some geodetic stations has been determined previously by two methods: (1) $\tau_L$ has been estimated from the geodetic group delays by fitting for the $A$ and $B$ coefficients in the equation above (D. MacMillan, 1993, unpublished); and (2) upper bounds on $|D_R|$, and therefore on $\tau_L$, have been calculated from $RL/RR$ fringe amplitude ratios measured in special experiments with dual-polarization stations (R. Potash, 1994, unpublished). Here, we describe the design, analysis, and preliminary results of observations carried out to determine the complex $D$ terms, not just upper limits on their magnitude, for a large number of geodetic stations.

Table 1. Stations and frequency sequences for July 1996 polarization sessions

| | **RDPLR1** | **NAPS2** | **GTRF11** | |
|---|---|---|---|---|
| *Stations* | FD-VLBA(Fd)<br>HN-VLBA(Hn)<br>KP-VLBA(Kp)<br>LA-VLBA(La)<br>OV-VLBA(Ov)<br>PIETOWN(Pt) | ALGOPARK(Ap)<br>GILCREEK(Gc)<br>NL-VLBA(Nl)<br>WESTFORD(Wf)<br>YLOW7296(Yk) | BR-VLBA(Br)<br>FORTLEZA(Ft)<br>HOBART26(Ho)<br>MK-VLBA(Mk)<br>SC-VLBA(Sc) | DSS65(65)<br>HARTRAO(Hh)<br>KASHIMA(Ka)<br>NYALES20(Ny) |
| *Freq. sequence* | 6 special | CDP-SX | DSNVLBA | |
| *# S/X freqs.* | 2 / 2 per seq. | 6 / 8 | 6 / 8 | |
| *S/X total span* | 128 / 722 MHz | 85 / 360 MHz | 100 / 360 MHz | |
| *Polarization* | RCP & LCP | RCP only | RCP only | |

## 2. The 1996 Polarization Experiments

On 22-23 July 1996, a special R&D experiment, RDPLR1, ran concurrently with two regular geodetic sessions, NAPS2 and GTRF11 — see Table 1 for some particulars. During each RDPLR1 scan, the six participating VLBA antennas recorded both polarizations at two S-band and two X-band frequencies. The RDPLR1 schedule had two distinct parts:

1. During the first eight hours, 3C84, OQ208, and 1308+326 were observed, with scans cycling through four different, dual-polarization, four-frequency sequences. The eight S- and eight X-band frequencies observed at the VLBA sites were selected to sample well the frequencies observed in the two geodetic sessions, and to include a few higher frequencies in each band.
2. During the remaining 16 hours, two of the RDPLR1 stations (Kp and La) were tagged along on NAPS2, and the other four (Fd, Hn, Ov, and Pt) were tagged along on GTRF11. In each session, the RDPLR1 stations alternated between two dual-polarization frequency sequences, for a total of four frequencies per band.

The observations with the RDPLR1 stations from all three sessions were processed at the MIT Haystack correlator. For most geodetic scans the SNR was expected to be too low to yield fringes for the cross-hands ($RL$) correlation; therefore only nine NAPS2 scans and 32 GTRF11 scans with high SNR were correlated.

## 3. Analysis

The analysis proceeded in two steps. First we estimated the VLBA $D$ terms from the data from part 1 of RDPLR1, and then we applied the results to the data from the geodetic sessions.

The method used to estimate the $D$ terms follows the procedure described in Section 4 of Roberts *et al.* [3] (see also [2]). We summarize the essential points here. For a radio source with no net circular polarization, the ratios between the cross-hands and parallel-hands ($RR$) visibilities may be written, to first order in the source fractional linear polarization and $D$ terms, as

$$\frac{R_1 L_2^*}{R_1 R_2^*} \;=\; G_2^* \, (\tilde{M}_{12} \, e^{-2i\phi_2} \;+\; D_{1R} \, e^{+2i(\phi_1 - \phi_2)} \;+\; D_{2L}^*) \qquad (3)$$

$$\frac{L_1 R_2^*}{R_1 R_2^*} \;=\; G_1\,(\tilde{M}_{21}^*\; e^{+2i\phi_1} \;+\; D_{1L} \;+\; D_{2R}^*\; e^{+2i(\phi_1-\phi_2)}) \tag{4}$$

where $G_i$ is the L/R ratio between the complex voltage gains for station $i$, $\tilde{M}$ is the complex fractional linear polarization of the source, and $D_{iL}$ is the RCP leakage term for the LCP feed. $G_i$ can be estimated from the parallel-hands visibility ratios $L_1 L_2^*/R_1 R_2^*$, provided there are three or more stations in a scan. (The $G_i$ phases cannot be determined unambiguously but must be referred to a reference station, which we chose to be Fd.) For 3C84 and OQ208, $|\tilde{M}|$ at centimeter wavelengths is $< 0.1\%$ [3], and the $\tilde{M}$ terms may consequently be ignored. The equations simplified in this manner are the basis for a linear least-squares solution for the unknown real and imaginary components of the $D$ terms. It is essential that the feed angle difference $\phi_1 - \phi_2$ vary in the data set, in order to break the degeneracies among the $D$-term components that would otherwise occur.

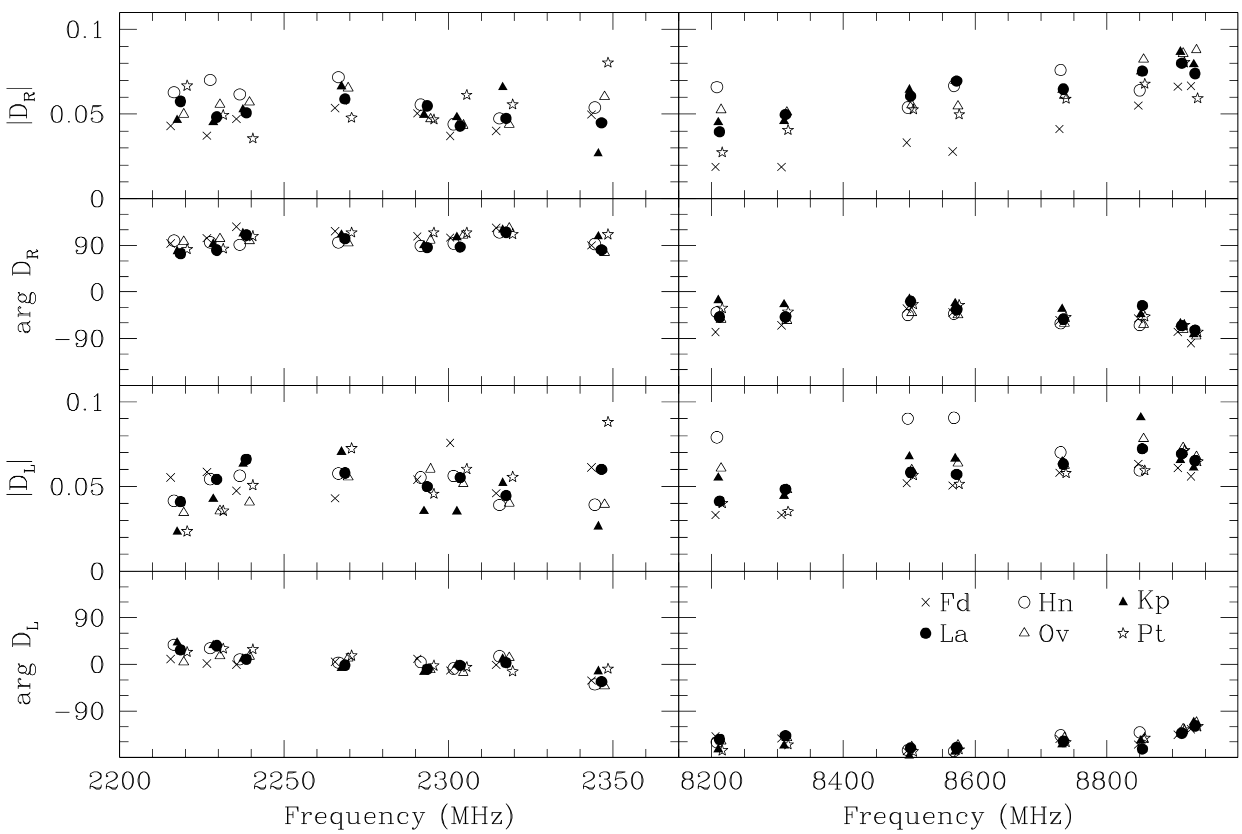


Figure 1. Frequency dependence of $D$ terms for RDPLR1 VLBA stations. In descending order from top: $D_R$ magnitude, $D_R$ phase (in degrees), $D_L$ magnitude, and $D_L$ phase. In each plot, the magnitude or phase is plotted for 6 stations at 8 frequencies; in order to reduce overlap, the plot symbols for different stations are offset slightly in frequency. Based on the repeatability of the results of the LSQ solutions with different data sets and methods of weighting, the standard error $\sigma$ in the real and imaginary components of $D$ is estimated to be 0.005-0.010; the corresponding errors in the magnitudes and phases are $\sigma$ and $\sigma/|D|$ radian, respectively. The uncertainties would have been signficantly lower but for a VLBA set-up problem that caused the loss of the first 100 minutes, during which the feed rotation angles were changing most rapidly.

Once the $D$ terms for the six dual-polarization stations are known, they can be applied to the results of the geodetic observations to estimate the $D$ terms for the NAPS2 and GTRF11 stations. During correlation, the "remote" station on each baseline (*i.e.*, station 2) was always a dual-polarization station. Using equation (3), one may then estimate the $D_{1R}$ term for the geodetic station by dividing the observed $RL/RR$ visibility ratio by the known (except for the reference $R-L$ phase at Fd) $G_2^*$ station gain ratio, subtracting the known quantity $D_{2L}^*$, and then counter-rotating by $2(\phi_1 - \phi_2)$. $\tilde{M}$ is assumed to be zero. Because some of the geodetic sources have fractional linear polarizations up to a few percent on VLBI scales, the results may be corrupted at this level. The hope is that, by averaging the $D$ terms over multiple sources and $(u,v)$ spacings, the error introduced by neglecting $\tilde{M}$ will be ~1% or less. Observations on the highly polarized quasar 1921-293 were excluded from the analysis.

## 4. Results

Figure 1 presents the $D$ terms estimated from the dual-polarization data acquired by the VLBA antennas on 3C84 and OQ208, during the first part of RDPLR1. In no case does the magnitude exceed 0.1 in voltage, or –20 dB in power. While the magnitudes often differ by a factor of 2-3 among the six stations, the phases are tightly clustered. The multiband error $\tau_L$ estimated from the $D_R$ terms has a maximum magnitude of 1.0±0.1 ps at X and 2.2±0.5 ps at S over all feed angles $\phi_1 - \phi_2$ and over all 15 VLBA-VLBA baselines.

The $D_R$ terms estimated for the non-RDPLR1 VLBA stations in NAPS2 and GTRF11 (*viz.*, Nl, Br, Mk, and Sc) in the second stage of the analysis are consistent with those in Figure 1.

The $D_R$ terms deduced for the non-VLBA geodetic antennas in NAPS2 and GTRF11 are generally larger than for the VLBA antennas, as shown in Figure 2. The S-band cross-polarization at Yk is particularly strong. The X-band cross-polarization at the four NAPS2 stations is generally $> -20$ dB. The fact that the X-band characteristics – especially the frequency dependence of the phase – at these four stations are similar is to be expected, as they use the same type of feed.

Table 2. S-band / X-band $\tau_L^{max}$ (ps) for baselines among four NAPS2 stations and for Kp-NAPS2 baselines

| | **Ap** | **Gc** | **Wf** | **Yk** |
|---|---|---|---|---|
| **Ap** | | 14 ± 4 / 5 ± 2 | 8 ± 2 / 9 ± 1 | 43 ± 7 / 8 ± 2 |
| **Gc** | | | 8 ± 3 / 4 ± 2 | 45 ± 12 / 2 ± 3 |
| **Wf** | | | | 24 ± 6 / 6 ± 2 |
| **Kp** | 4 ± 2 / 6 ± 1 | 8 ± 2 / 5 ± 1 | 3 ± 1 / 7 ± 1 | 14 ± 4 / 9 ± 1 |

Table 2 lists the maximum magnitude of $\tau_L$ calculated over all $\phi_1 - \phi_2$ for the baselines among the four NAPS2 stations in Figure 2, and for the baselines between a representative VLBA station, Kp, and the NAPS2 stations. (For weak cross-polarization, $\tau_L^{max}$ is simply the root-sum-square of the $A$ and $B$ coefficients in equation (2).) The similarity in the frequency dependence of the X-band $D_R$ phases among the NAPS2 stations is largely responsible for the relatively small values of $\tau_L^{max}$ on the NAPS2 baselines: because the argument of $D_{1R}D_{2R}^*$ is small, the frequency dependence of the argument of equation (1) is reduced from what it otherwise might be. Indeed, it is the difference in the X-band $D_R$ phase characteristics between Kp and the NAPS2 stations that causes $\tau_L^{max}$ on the Kp baselines to have values in the same range as those on the internal NAPS2 baselines

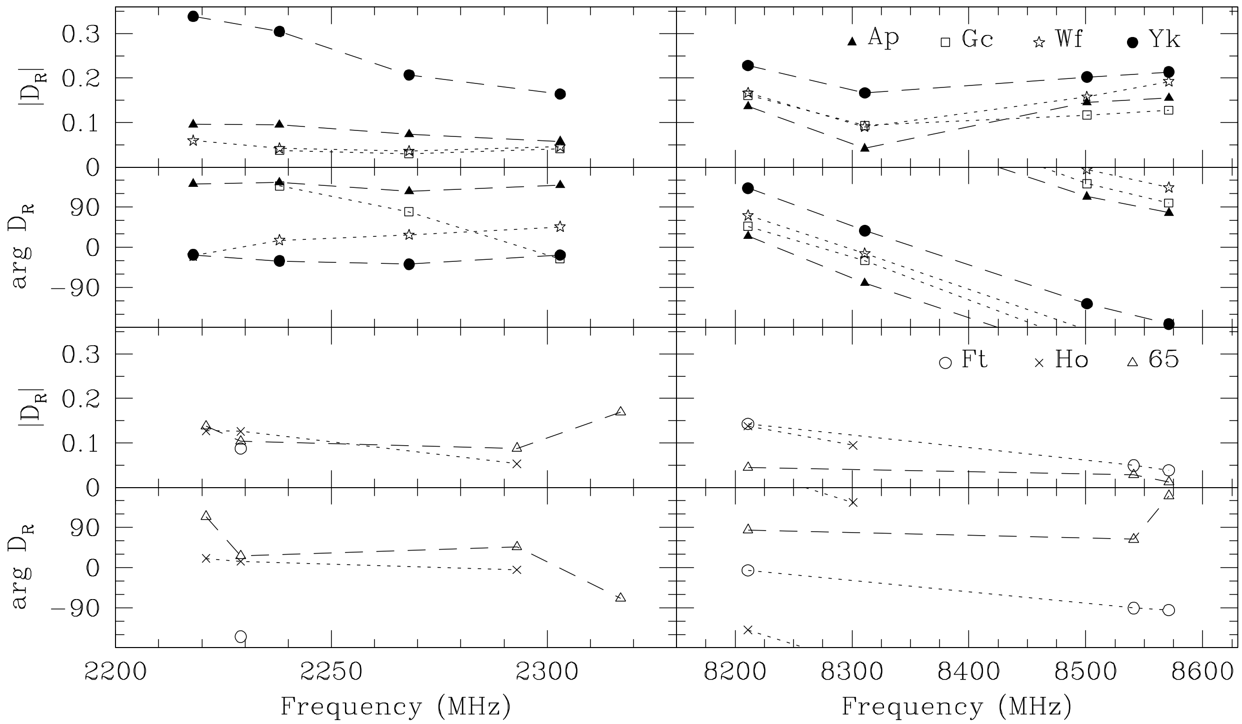


Figure 2. Frequency dependence of $D_R$ for selected geodetic stations. Top plots show the magnitude and phase (in degrees) for four NAPS2 stations, and the lower plots do the same for three GTRF11 stations. Each point represents the mean of $\geq 2$ $D_R$ estimates ($\geq 5$ in most cases) from different scans or different baselines. Based on the rms scatter of $\leq 0.03$ in the real and imaginary components, the standard errors $\sigma$ in these components are estimated to be 0.01-0.02; the corresponding errors in the magnitude and phase are $\sigma$ and $\sigma/|D_R|$ radian, respectively.

despite the much smaller $|D_R|$ magnitudes for Kp.

Because the NAPS2 $D$ terms are available at only four frequencies, the values in Table 2 should be considered only illustrative of what $\tau_L^{max}$ would be in a geodetic session with more, or different, frequency channels, especially if the new frequency sequence spans a wider RF bandwidth.

## References


[1] Herring, T.A., Precision and Accuracy of Intercontinental Distance Determinations Using Radio Interferometry, Ph.D. thesis, MIT, 1983.

[2] Massi, M., G. Comoretto, M. Rioja, G. Tofani, Baseline Errors on European VLBI Network Measurements: II. Instrumental Polarization, Astron. Astrophys. Suppl., **116**, 167-176, 1996.

[3] Roberts, D.H., J.F.C. Wardle, L.F. Brown, Linear Polarization Radio Imaging at Milliarcsecond Resolution, Astrophys. J., **427**, 718-744, 1994.

[4] Rogers, A.E.E., Instrumentation Improvements to Achieve Millimeter Accuracy, in Proceedings of the AGU Chapman Conference on Geodetic VLBI: Monitoring Global Changes, NOAA Technical Report NOS 137 NGS 49, 1-6, 1991.